Dear Editor,
Please find attached the revised manuscript and author response to the reviewers' comments of the manuscript "Hydrological characterization of cave drip waters in a porous limestone: Golgotha Cave, Western Australia" by Mahmud et al. for your consideration. We believe we have addressed all questions raised by the two reviewers of the manuscript.

As requested, we have included a detailed response to reviewer's questions (below), indicating page and line numbers where the changes are made in the revised manuscript. A marked-up manuscript version is also provided showing all the modifications.

If you have any additional questions, we would be more than happy to address them.

With kind regards,

For the authors,
Kashif Mahmud

Comments to the Author
Interactive comment on "Hydrological characterization of cave drip waters in a porous limestone: Golgotha Cave, Western Australia" by Mahmud et al.

Reviewer(s) Comments:
Anonymous Referee #1
In the submitted manuscript Mahmud et al. provide a detailed study on the dynamics of cave drips at a large karst cave in South West Australia. The authors use a large set of automatically recorded drip rate records to classify and cluster the different drips by their statistical properties and knowledge from previous research. They show that established classification schemes do not apply to their data set but their new clustering method provided a clear distinction of 4 clusters of drip types within the cave. The most prominent one, cluster 1, consisted of drips that were mostly controlled by matrix flow, which is in accordance with previous classification using LiDAR imaging. The other clusters were expressed by a stronger hydrological variability in terms of mean discharge and flow variability.

We appreciate the reviewer's comments.

The manuscript is generally well-written, the methods are clearly explained and the conclusions are well supported by the results and discussion. Some improvement is necessary in terms of structure and detail: Some parts of the methods appear in the results section and should be moved to the methods description. Also the elaborations about the drip characteristics are a bit too detailed and may be shortened to improve the readability of the manuscript.

We have reorganized the method/result sections and removed the unnecessary portion that described the previous paper (see the newly structured section 3 and 4).

Finally, another subsection addressing the impact of the results of this study would be very valuable for the karst and cave hydrology communities. I am confident that this can be done in the frame of minor revisions.

The impacts of the findings of this study have been briefly identified in the last paragraph of the conclusion, however we have elaborated this discussion further, including presenting a summary of the implications of the current study, as well as bringing together an overall summary tying in the relevant findings from the previous two papers by Mahmud et al. We have also recommended potential future research directions. This appears as the following subsection in the revised manuscript (section 5):

Implications of the findings and future research:

We will emphasize the overall impacts of this study from different perspectives, starting with temporal analysis, multisite analysis, karst modelling, and then paleoclimate records.

Starting with the time-series analysis, this research presents a methodology that can be applied globally for drip logger data. The results show that some data-integration is necessary to avoid artefacts from slow drip sites. For sites where there is significant matrix flow, our study has demonstrated that the Smart and Friederich (S&F) classification is not appropriate. Therefore, this study proposes an alternative hydrological classification scheme that incorporates cave sites influenced by matrix flow. The times series approach adopted in this study also opens the way for improved analysis and classification of hydrology time series in general e.g. tests for non-linearity, autocorrelation, cluster analysis, etc. and all of these will certainly benefit our understanding of the hydrology of karst systems.

In this study, we also extend the analysis of drip time series to multiple sites, whereby we take advantage of the ensemble of loggers to extract common properties by clustering, which would not be possible with single site analysis. The results show that by considering multiple simultaneous time series, one can make better inferences about water flow and unsaturated zone properties. The main impact is to recommend the use of spatial networks of loggers over individual loggers – it should be noted that currently, most researchers deploy only a few loggers to understand the flow to individual sites. This study also proposes a possible methodology for the analysis of such datasets.

Regarding application of our findings, we believe that our methodology based on drip logger datasets can provide direct evidence of deep drainage, and therefore the timing of diffuse recharge, which could be used for basic model calibration. Spatial drip data (possibly combined with Lidar) is beneficial to infer flow types (e.g. the proportion of fracture vs matrix, etc.) which could be used for model configuration to produce realistic karst recharge (Hartmann et al. 2012), and hence large-scale groundwater estimation (Hartmann et al. 2015). Another potential application is the integration of flow types in groundwater models through inverse modelling. Such data could also be used to constrain water isotope model configurations used for forward modelling speleothem $\delta^{18}O$ (Bradley et al. 2010, Treble et al. 2013). Overall, the findings of this work will definitely provide a better understanding of processes that control vadose zone flow and transport processes, which would ultimately help develop approaches to incorporate these processes into simulation models (Hartmann and Baker 2017).

The analysis, presented here and combined with the findings of our previous two papers (Mahmud et al. 2016, Mahmud et al. 2015), provides valuable information for

paleoclimatologists and geochemists wishing to sample stalagmites. While these studies have characterised Golgotha Cave, they could be applied to any other cave system globally. We can summarize our previous work as follows: 1) we have devised a classification for flow-type based on stalactite morphology (Mahmud et al. 2015); 2) quantified the recharge response of each flow type to infiltration (Mahmud et al. 2016); 3) combined findings in points 1-2 to estimate the total volume of cave discharge; 4) compared cave discharge with infiltration to estimate the total recharge volume and identify highly focused areas of recharge (Mahmud et al. 2016). The current study has further developed the spatial and temporal statistical relationships between the flow sites, permitting both quantification and visualisation of the hydrology between the ground surface and the cave ceiling. More generally, these studies illustrate the heterogeneity between flow sites and what causes this, as well as putting forth methods that can be applied to any cave system to better understand diffuse recharge and paleoclimate records from speleothems.

We have further proposed some ideas for future research that have evolved from this study. For example:

a) Combining drip logger network with a surface weather station and soil moisture network to constrain the water balance with site specific measurements using modelled input time series derived from nearby meteorological stations. Additionally, employing sap flow meters to constrain tree water use.
b) Combining the logger network, which constrains diffuse recharge, to a bore network that measures groundwater level, to understand the relative importance of diffuse and river recharge.
c) Combining cave drip logger data with surface geophysics data to track water movement.

Please see the attached and commented pdf for more detailed specific and technical comments.

1) Line 27: The typo

This typing mistake is now corrected (line 26).

2) Line 50: The typo

A comma is added (line 53).

3) Line 54: This may depend on the more or less developed connection between the surface and the cave, doesn't it?

Yes indeed, is added (line 57-58).

4) Lines 57-58: remove unnecessary brackets

Removed (line 61-62).

5) Line 131: Provide short information about method.

This paper is essentially not about climate, and is about drip categorization. So, we have removed the entire paragraph explaining water budgets and infiltration, and focused only on drip classification (section 2.2).

6) Line 139: The second part of this section is a bit too detailed, please shorten.

We have immensely minimized the description of previous works (see section 2.3).

7) Line 160: better use points instead of lines to avoid misinterpretation

We think point plots would make it difficult to grasp the trend of these dense time series, and hence we prefer to stick with the line plots.

8) Line 216: which processes does the offset account for? different flow lengths? Please provide short explanation.

The offset *O* (in hours) is needed to align two time-series such that they present maximum correlation. This offset accounts for the lag time based on the maximum correlation between two-time series in order to match those time series. This is explained in line 222-223.

9) Line 223: Please provide some short description of the MDS method for readers that are not familiar with the method.

Multi-dimensional scaling (MDS) starts by defining a distance between a set of objects. In our case, each drip logger is an object and a specific distance between drip loggers is considered to characterize the similarity between any two loggers. This definition with more elaboration on the technique is added in section 3.2.

10) Line 248: please move apart the 10^4 and the figure title, please provide x- and y-axis labels

The figure Y-axis ticks is modified, however we feel adding the axis levels to each of the subplots will make the diagram congested. So, we have added the axis labels in the first plot with a description in the figure caption (Figure 3).

11) Line 262: Same as above: figure needs axis labels

We have moved this figure to supplementary section S1. Similar to the previous comment, we feel adding the axis levels to each of the subplots will make the diagram congested. So, we have added the axis labels in the first plot with a description in the figure caption (Figure S2).

12) Lines 268-269: Please mention in methods that this is part of the analysis.

Mentioned in method section 4.1 (line 187-189).

13) Line 283: please mention in caption that ln is the log10 (isn't it?)

Yes it is, cited in axis labels (Figure 2).

14) Line 292, 295: here, and some lines before some accidental breaks should be removed

Removed (see section 4.4).

15) Line 306: K-means requires a pre-definition of the number of clusters. How was this done here?

We have defined the cluster number in section 3.2 (line 245) based on the number of flow categories identified by Mahmud et al. (2016).

16) Line 316: or their flow paths pass the same hydrological domain, the karst matrix.

That could be another possibility and therefore is added in line 337-338.

17) Line 332: Another subsection discussing the implications of this research concerning the understanding of cave hydrology, karst recharge, and paleoclimate reconstruction is missing

here. Also, how the newly gained knowledge could be incorporated into hydrological models to simulate the unsaturated zone (see refs below) would be very valuable.

Bradley, C., Baker, A., Jex, C.N. & Leng, M.J. 2010. Hydrological uncertainties in the modelling of cave drip-water δ18O and the implications for stalagmite palaeoclimate reconstructions. Quaternary Science Reviews, 29, 2201–2214, doi: 10.1016/j.quascirev.2010.05.017.

Treble, P.C., Bradley, C., et al. 2013. An isotopic and modelling study of flow paths and storage in Quaternary calcarenite, SW Australia: Implications for speleothem paleoclimate records. Quaternary Science Reviews, 64, 90–103, doi: 10.1016/j.quascirev.2012.12.015.

Hartmann, A., Lange, J., Weiler, M., Arbel, Y. & Greenbaum, N. 2012. A new approach to model the spatial and temporal variability of recharge to karst aquifers. Hydrology and Earth System Sciences, 16, 2219–2231, doi: 10.5194/hess-16-2219-2012.

Hartmann, A., Gleeson, T., Rosolem, R., Pianosi, F., Wada, Y. & Wagener, T. 2015. A large-scale simulation model to assess karstic groundwater recharge over Europe and the Mediterranean. Geoscientific Model Development, 8, 1729–1746, doi: 10.5194/gmd-8-1729-2015.

> Earlier in this response letter we have mentioned adding a new section with all these suggested references. This section 5 discusses the implications of this research concerning the understanding of cave hydrology, karst recharge, modelling, and paleoclimate reconstruction.

Reviewer(s) Comments:

Anonymous Referee #2

This manuscript is a follow up on drip monitoring data that were published in previous works including a 2016 paper in HESS. Whereas classification of flow regimes in the previous paper(s) was based also on morphological characteristics of the stalactites, here a similar clustering is based solely on a cluster analysis of the drip data. Beside the cluster analysis, there are new histograms and analysis of autocorrelation, which may add some qualitative understandings of the karst flow regime in these stalactites (seasonality, annual precipitation variability). I am not sure the "delta" from the previous works on this data that is presented in the current manuscript is worth a new HESS paper. I am sure that in the present way it is written it is not. Therefore, I recommend on a major revision in which: 1) the description of previous methods and results will be decreased to minimum; 2) Elaboration on the new statistical methods and results that are used here, 3) the presentation and discussion concerning the histograms and autocorrelation analysis will be upgraded significantly; and 4) the "delta" from our understanding of the system we had before this analysis will be declared more explicitly.

> We have removed the unnecessary portions that described the previous paper and elaborated the result section significantly with the description of new statistical analysis (see the newly structured section 2.3 and 3). We have also added a section about the wider impacts of the research in the field of karst and cave hydrology that distinguishes the added findings compared to our previous works in this domain (see the newly added section 5). The site description and methods are stripped to the

minimum during the revision and substantially revised, and this makes space for increased discussions and presentation of the results.

Major Comments

1) Even though it is declared in the manuscript and figure captions, it's inappropriate that more than half of the paper including 3 figures and 2 tables are repetition of methods and results of a previous work. It doesn't look good, especially the almost identical figures, avoid.

We have removed Figure 2 completely and cited our previous work (Mahmud et al. 2016) for the climate data and drip time series. Figure 3 is merged with Figure 1 by focusing only the cave floor images, complementing with the ceiling image and photographs of underlying stalagmites shown in Fig. 3 of previous paper (Mahmud et al. 2016). We have significantly modified the tables (Table 1 and 2) to represent the new findings with minimal overlap of previous outcomes.

2) Lines 83-212, old stories, to be reduced to a 1/3 of current.

We have condensed the content more and emphasized on our previous works (Mahmud et al. 2016, Mahmud et al. 2015) to follow for more detail. See the newly structured section 2 and 3.

3) Lines 213-228 these are the new methods: Elaborate in explaining them, equations, figures that illustrate, etc,. MDS, K-means, these are not general statistics (this section (4) has to be as long as sections 2+3 at least).

We employed a data analysis technique called Multi-dimensional scaling (MDS), that allows a data dimensionality reduction i.e., mapping complex multidimensional data on a low-dimensional manifold. MDS is a technique concerned with embedding a set of points in a low-dimensional space so that the distances between the points resemble as closely as possible a given set of dissimilarities between objects that they represent (Birchfield and Subramanya 2005). MDS requires a distance matrix to be computed, in which a single scalar number characterizes the similarity between any two time-series. It takes an input matrix giving dissimilarities between pairs of items and outputs a coordinate matrix whose configuration minimizes a loss function. MDS is also known as Principal Coordinates Analysis (PCoA) and works differently from principle-component analysis (PCA), which operates on a covariance matrix, MDS operates on a distance or dissimilarity matrix (Pisani et al. 2016). Even if PCA and MDS methods can return the same results in specific contexts, MDS can be considered as a more general method that maintains its validity in a rigorous sense also for non-euclidean distances, i.e., the distance matrix (d) chosen in this study. MDS is used to translate these distances into a configuration of points defined in an n-dimensional Euclidean space (Cox and Cox 1994). A MDS results in a set of points arranged so that their corresponding Euclidean distances indicate the dissimilarities of the time series.

The basic steps of performing the MDS algorithm are:

1. Construct the distance matrix d: One key component in clustering is the function used to measure the temporal similarity (or distance) between any two time-series being compared. To define an appropriate measure of similarity between time series, we determine two factors: firstly, the offset (O) to match two time-series based on their maximum correlation, and secondly the complement of the correlation coefficient (1-R) between the time series (Jex et al. 2012). Initially, we compute the cross-correlation function and O is defined as the lag time based on

the maximum correlation between two time-series. Next, we define R as the correlation coefficient with the time series being moved by the offset amount *O* to have maximum correlation coefficient. Finally, the distance matrix (*d*) is computed for each pair of loggers using the following equation (Jex et al. 2012):

$$d = O\,(1 - R)$$

2. Compute the inner product matrix $\mathrm{B} = -\frac{1}{2}JDJ$, where $\mathrm{J} = I - \frac{1}{n}\mathbf{1}\mathbf{1}^T$ is the double-centering matrix and $\mathbf{1}$ is a vector of all ones.
3. Decompose B as $\mathrm{B} = V\Lambda V^T$, where $\Lambda = \mathrm{diag}\,(\lambda_1, \ldots, \lambda_n)$, the diagonal matrix of eigenvalues of B, and $\mathrm{V} = [\mathrm{v}_1, \ldots, v_n]$, the matrix of corresponding unit eigenvectors. Sort the eigenvalues in non-increasing order: $\lambda_1 \geq \cdots \geq \lambda_n \geq 0$.
4. Extract the first p eigenvalues $\Lambda_p = \mathrm{diag}\,(\lambda_1, \ldots, \lambda_p)$ and corresponding eigenvectors $\mathrm{V}_p = [v_1, \ldots, \mathrm{v}_p]$.
5. The corresponding Euclidean distances of the set of points, indicating the dissimilarities of the time series are now located in the $n \times p$ matrix $\mathrm{X} = \left[x_1, \ldots, \mathrm{x}_p\right]^T = \mathrm{V}_p {\Lambda_p}^{1/2}$.

The k-Means clustering algorithm is then used to divide these points into k clusters, which corresponds to a categorization of the drip data time series. k-means clustering, or Lloyd's algorithm (Lloyd 1982), is a method of vector quantization that is popular for cluster analysis in data mining. k-means clustering aims to partition n observations into k clusters in which each observation belongs to the cluster with the nearest mean, serving as a prototype of the cluster.

The algorithm proceeds as follows:

1. Choose *k* initial cluster centers (*centroid*): Here, we use *k*=4 clusters as this was the number of flow categories identified by Mahmud et al. (2016).
2. Compute point-to-cluster-centroid distances of all observations to each centroid. There are two steps to follow: first assign each observation to the cluster with the closest centroid. Then individually assign observations to a different centroid if the reassignment decreases the sum of the within-cluster, sum-of-squares point-to-cluster-centroid distances.
3. Compute the average of the observations in each cluster to obtain *k* new centroid locations.
4. Repeat steps 2 and 3 until cluster assignments do not change, or the maximum number of iterations is reached.

All these are added in the manuscript (section 3.2).

4) What does the MDS analysis add to the correlation matrices analyzed in Mahmud et al. 2016. ?

This paper goes beyond the analysis done by Mahmud et al. (2016), where the correlation was considered without offset, and the quantitative drip data were not used for clustering, but only for validation. We could summarize both the papers like below in terms of investigating the dependence between multiple drip time series:

Mahmud et al. (2016): correlation between time series
Mahmud et al. (2017): computation of a distance between time series + offset correction + MDS-based clustering

Overall this study establishes a novel way to find consistent characterization of cave hydrology, which can be obtained by performing together both methodologies of Mahmud et al. (2015) and Jex et al. (2012). It relies on a metric that defines drip logger time series as similar if they are well correlated and only have a small offset with one another, and therefore these time series should cluster together. The MDS analysis supports this hypothesis and moreover, displays the spatial patterns of the flow paths between the surface and the cave chambers. This technique shows potential to classify, quantify and visualise the observed relationships between infiltration through the fractured limestone rocks and surface climate inputs.

Specific Comments

5) L 22 –Abstract should not include references.

Removed (line 30-31).

6) L 27 Capital C

Corrected (line 26).

7) L 37 for development of karst in relation to fractures, beds, bedding plains see also Kurtzman et al., 2009, Geosphere, v. 5; no. 2; p. 126–139;

The reference is added in line 39.

8) Line 91 "high matrix porosity" – give numbers 0.1? 0.2? 0.3?

The porosity is reported in Smith et al. (2012) as 0.3 – 0.5 and is added in line 96.

9) Lines 215-221: define cross-correlation function; is O and R calculated to all n(n-1)/2 pairs of drip data, elaborate, explain the method. End of lines 216 and 218 – redundancy. What are the dimensions of the distance matrix – d?

Cross-correlation is a measure of similarity of two time-series as a function of the displacement of one relative to the other. The function is an estimate of the covariance between two time-series, y_{1t} and y_{2t}, at lags $k = 0, \pm1, \pm2, ...$

Yes, both O and R are calculated to all n(n-1)/2 pairs of drip data. We will reorganize this section with detailed explanation on both MDS and K-means algorithms, as we stated before in comment 3.

The distance matrix d is square, symmetric, and has dimension equal to the number of drip loggers. All these are added in section 3.2.

10) Lines 223 – 228, what is MDS? Is it of the family of the classic principle-component analysis (PCA)? In the current application how many dimensions? Equations, figures, tell us the method? What is the K-means algorithm – elaborate on top of citing?

We have discussed above the MDS and k-means algorithm earlier in this response letter and is explained in details in the revised manuscript (section 3.2).

11) Figure 4. Put all vertical axis the same - 10000 or 1X10-4, do not mix; Color choice not good – try blue for wet seasons ad red for dry, or rainy 2013 in contrast with other play with it and choose the better, print and see if it is good on printing as well.

Y-axis ticks are modified as well as different colour choices are explored to find the best one in Figure 3.

12) L 245. These histograms are not skewed. Maye be add a sub figure to figure 4 with the most characteristic normal, skewed, be-modal histograms, including a continuous line of the pdf to illustrate.

The histogram plots were not clearly explained and are improved in the revised manuscript (see section 4.2).

We believe that adding a subplot is not necessary at all, because there was a silly mistake in the text (mentioning wrong sites as skewed distribution) in earlier submitted version, which made the reviewer to ask for these extra figures. We have corrected the text and would prefer to leave the layout like this without making it too clumsy.

13) Figure 5 and relevant text. – The most contrasting ACF are usually at time lag of 150-200 (1 season in the 2-seasons Mediterranean climate), I would plot these ACF until lags of 365 days to enhance the seasonal understanding, that may be gained.

We have moved this section to supplementary material section S1. We tested the ACFs until lags of 365 days, however in general the yearly signal is quite weak. In some drips, we got some negative correlation, but it is very insignificant and no process can explain that negative yearly correlation. This is now mentioned in section S1.

14) Figure 6 and 7, choose more contrasting colors and increase symbol size.

Contrasting colors are used with larger symbol size (Figure 2 and 4).

15) L 292 and 296 typo mistake of new line.

Corrected (section 4.4).

16) L313-314 “inconsistency” - unclear

We observe that the clustering generally agrees with the morphology-based flow classification of our previous work (Mahmud et al. 2016) with few exceptions. For example, site 2vi has really high discharge with high variability, showing irregular drip rate. This is clarified in line 331-333.

17) L339 the beginning of line is unclear

The histogram distributions of various drip data time series can illustrate the differences between the flow classifications. This is now clarified in line 408-410.

Additional references:

Birchfield, S.T. and Subramanya, A. (2005) Microphone Array Position Calibration by Basis-Point Classical Multidimensional Scaling. IEEE Transactions on Speech and Audio Processing 13(5), 1025-1034.

Bradley, C., Baker, A., Jex, C.N. and Leng, M.J. (2010) Hydrological uncertainties in the modelling of cave drip-water δ18O and the implications for stalagmite palaeoclimate reconstructions. Quaternary Science Reviews 29(17-18), 2201-2214.

Cox, T. and Cox, M. (1994) Multidimensional scaling, Chapman and Hall, London.

Hartmann, A. and Baker, A. (2017) Modelling karst vadose zone hydrology and its relevance for paleoclimate reconstruction. Earth-Science Reviews 172, 178-192.

Hartmann, A., Gleeson, T., Rosolem, R., Pianosi, F., Wada, Y. and Wagener, T. (2015) A large-scale simulation model to assess karstic groundwater recharge over Europe and the Mediterranean. Geosci. Model Dev. 8(6), 1729-1746.
Hartmann, A., Lange, J., Weiler, M., Arbel, Y. and Greenbaum, N. (2012) A new approach to model the spatial and temporal variability of recharge to karst aquifers. Hydrol. Earth Syst. Sci. 16(7), 2219-2231.
Jex, C.N., Mariethoz, G., Baker, A., Graham, P., Andersen, M., Acworth, I., Edwards, N. and Azcurra, C. (2012) Spatially dense drip hydrological monitoring and infiltration behaviour at the Wellington Caves, South East Australia. International Journal of Speleology 41(2), 283–296.
Lloyd, S. (1982) Least squares quantization in PCM. IEEE Transactions on Information Theory IT-28(2 pt 1), 129-137.
Mahmud, K., Mariethoz, G., Baker, A. and Treble, P.C. (2017) Hydrological characterization of cave drip waters in a porous limestone: Golgotha Cave, Western Australia. Hydrol. Earth Syst. Sci. Discuss. 2017, 1-19.
Mahmud, K., Mariethoz, G., Baker, A., Treble, P.C., Markowska, M. and McGuire, L. (2016) Estimation of deep infiltration in unsaturated limestone environments using cave LiDAR and drip count data. Hydrol. Earth Syst. Sci. 20, 359-373.
Mahmud, K., Mariethoz, G., Pauline, C.T. and Baker, A. (2015) Terrestrial Lidar Survey and Morphological Analysis to Identify Infiltration Properties in the Tamala Limestone, Western Australia. Selected Topics in Applied Earth Observations and Remote Sensing, IEEE Journal of 8(10), 4871 - 4881.
Pisani, P., Caporuscio, F., Carlino, L. and Rastelli, G. (2016) Molecular Dynamics Simulations and Classical Multidimensional Scaling Unveil New Metastable States in the Conformational Landscape of CDK2. PLoS ONE 11(4), 1-22.
Smith, A.J., Massuel, S. and Pollock, D.W. (2012) Geohydrology of the Tamala Limestone Formation in the Perth Region: Origin and Role of Secondary Porosity, p. 63.
Treble, P.C., Bradley, C., Wood, A., Baker, A., Jex, C.N., Fairchild, I.J., Gagan, M.K., Cowley, J. and Azcurra, C. (2013) An isotopic and modelling study of flow paths and storage in Quaternary calcarenite, SW Australia: implications for speleothem paleoclimate records. Quaternary Science Reviews 64(0), 90-103.

Hydrological characterization of cave drip waters in a porous limestone: Golgotha Cave, Western Australia

Kashif Mahmud[1], Gregoire Mariethoz[2], Andy Baker[3], Pauline C. Treble[4]

[1]Hawkesbury Institute for the Environment, Western Sydney University, Australia
[2]Institute of Earth Surface Dynamics, University of Lausanne, Switzerland
[3]Connected Waters Initiative Research Centre, UNSW Australia, NSW, Australia
[4]Australian Nuclear Science and Technology Organisation, Lucas Heights, NSW, Australia

Correspondence to: Kashif Mahmud (k.mahmud@westernsydney.edu.au)

Abstract

Cave drip water response to surface meteorological conditions is complex due to the heterogeneity of water movement in the karst unsaturated zone. Previous studies have focused on the monitoring of fractured rock limestones that have little or no primary porosity. In this study, we aim to further understand infiltration water hydrology in the Tamala Limestone of SW Australia, which is Quaternary aeolianite with primary porosity. We build on our previous studies of the Golgotha Cave system and utilize the existing spatial survey of 29 automated cave drip loggers and a LiDAR-based flow classification scheme, conducted in the two main chambers of this cave. We find that a daily sampling frequency at our cave site optimizes the capture of drip variability with least possible sampling artifacts. With the optimum sampling frequency, most of the drip sites show persistent autocorrelation for at least a month, typically much longer, indicating ample storage of water feeding all stalactites investigated. Drip discharge histograms are highly variable, showing sometimes multimodal distributions. Histogram skewness is shown to relate to the wetter than average 2013 hydrological year and modality is affected by seasonality. The hydrological classification scheme with respect to mean discharge and the flow variation, can distinguish between groundwater flow types in limestones with primary porosity, and the technique could be used to characterize different karst flow paths when high-frequency automated drip logger data are available. We observe little difference in the coefficient of variation (COV) between flow classification types, probably reflecting the ample storage due to the dominance of primary porosity at this cave site. Moreover, we do not find any relationship between drip variability and discharge within similar flow type. Finally, a combination of multi-dimensional scaling (MDS) and clustering by k-means is used to classify similar drip types based on time series analysis. This clustering reveals four unique drip regimes which agree with previous flow type classification for this site. It highlights a spatial homogeneity in drip types in one cave chamber, and spatial heterogeneity in the other, which is in concordance with our understanding of cave chamber morphology and lithology.

Keywords: karst aquifers, drip loggers, infiltration, cave drip water

1 Introduction

Karst features in limestone are typically developed from the solutional dissolution of fractures and bedding planes in carbonate rocks (Arbel et al., 2010; Kurtzman et al., 2009). Worldwide, karst regions represent significant geographical areas with potentially high rates of infiltration through fractured and karstified carbonate rocks. The most usual recharge method in karstic aquifers is the faster infiltration through the deep karstic openings (Ford and Williams, 2007). Complex spatial spreading of various karst features such as solutionally widened fractures, caves and conduits, makes the monitoring and precise groundwater recharge modeling very difficult (Lange et al., 2003; Arbel et al., 2010). The upper part of karstified rock (the epikarst zone) has higher permeability than the underlying vadose zone (Klimchouk, 2004). Therefore, infiltration into the epikarst zone is faster compared to the drainage through it, and water is kept stored in this region. This stored water in the vadose zone seeps slowly and finally emerges inside caves as infiltrating drip waters (Williams, 1983).

Karstic features such as speleothems, commonly used to reconstruct paleo-environmental records, are formed due to calcite deposition from cave drip water. Therefore, the knowledge of drip water hydrology is critical to study the paleoclimatic records (Baldini et al., 2006). An early study using tipping bucket loggers formulated a relationship between maximum discharge and coefficient of variation of discharge to categorize cave discharges (Smart and Friederich, 1987), for a fractured-rock limestone system with a vertical range of approximately 140 m (GB Cave, Mendip Hills, UK). They found that the drips close to the surface have extreme coefficient of variations, whereas the drips in depths have fairly constant flow rates over time, with a significant possibility of water storage in vadose zone fractures. Thus the stalagmite record resulting from slower drips may be more closely related to the karst hydrology rather than palaeoclimate (Baldini et al., 2006). This may also be a consequence of the developed connection between the surface and the cave. Quantitative analysis of such stalagmite drip data has, in the past, used manual observations of cave drips (e.g. Baker et al 1997). However, the recent development of automatic cave drip loggers (Collister and Mattey, 2008) has enabled the generation of high temporal resolution and continuous drip discharge time-series (e.g. (Jex et al., 2012; Cuthbert et al., 2014; Markowska et al., 2015; Mariethoz et al., 2012)), providing new opportunities for quantitative hydrological analysis.

Here we present monitoring data from Golgotha Cave located in SW Western Australia that has been extensively monitored since 2005, with the aim of better understanding karst drip water hydrogeology and the relationship between drip hydrology and surface climate. We build on the work of Mahmud et al. (2016), which presented the largest spatial and temporal survey of automated cave drip monitoring with matrix (primary) porosity published to date. This previous study consisted of data from two large chambers within this cave, measured in the period from August 2012 to March 2015, using a highly spatially (29 sites in two separate chambers) and temporally (0.001 Hz, 15 min intervals) resolved dataset and developed a recharge estimation technique for caves using the drip data and flow classification techniques of Mahmud et al. (2015a). Mahmud et al. (2015a) performs morphological analysis of karstic features, based on ground-based LiDAR data, to identify

different flow processes in karstified limestone. Based on the findings of Mahmud et al. (2015a); Mahmud et al. (2016), here we investigate the relationship between drip water hydrology and cave depth, spatial location and stalactite type, and develop a hydrological classification scheme that is appropriate to high-frequency drip logger data and limestones with a primary porosity. This classification scheme is also compared with previous studies (Smart and Friederich, 1987; Baker et al., 1997) to examine the limitations of these previous schemes. These findings will also help better characterize and understand water movement in highly porous karst formations.

Finally, we use a combination of multi-dimensional scaling (MDS) and the popular K-Means algorithm for clustering similar drip characteristics. Time series clustering has been shown to be effective in providing useful information in various domains (Liao, 2005) and is implemented here to determine the degree of similarity between two drip time series. There seems to be an increased interest in time series clustering as part of the research effort in temporal data mining. The method we use here is suitable for large datasets, has been studied extensively in the past and achieves good results with minimum computational cost (Jex et al., 2012; Scheidt and Caers, 2009; Borg and Groenen, 1997).

2 Site Description

2.1 Studied Cave

The cave site has been explained in detail by Mahmud et al. (2015a); Mahmud et al. (2016); Treble et al. (2013). Briefly, the field site, Golgotha Cave is 200 m in length and up to 25 m in width (Figure 1), is developed in Quaternary aeolianite, which consists of wind-blown calcareous sands that were deposited along the southwest coast of Australia (Brooke et al., 2014). Vadose zone water flow, and subsequent widening by ceiling collapse, formed the cave chambers. Treble et al. (2013) described the cave site as being developed in the Spearwood System of the Tamala Limestone and is mantled by a variable thick layer of sand formation having depths of between 0.3 m and 3 m. Diffuse (or matrix) flow is likely to be dominant in the Tamala Limestone formation due to its high matrix porosity as 0.3 – 0.5 (Smith et al., 2012). Karst in this region is also called “syngenetic” (Treble et al., 2013) that implies processes like preferential vertical dissolution and varying morphology of the subsurface caprock. These processes may establish vadose-zone preferential flow extending to the cave ceiling, with occasional rapid delivery of percolating waters deep into the calcarenite which end up seeping through to the cave ceiling. Therefore, this young limestone formation offers various opportunities for preferential flow into the hostrock and storage within it (Brooke et al., 2014). Golgotha Cave was chosen because (a) it is located in an intensively studied karst area (Mahmud et al., 2015a; Mahmud et al., 2016; Treble et al., 2015; Treble et al., 2013; Treble et al., 2016), which has over ten years of manual and 3 years of automated drip water monitoring, (b) it contains actively growing speleothems, and (c) it is accessible year-round.

Based on the findings of Treble et al. (2013) and the morphological analysis of stalactite clusters by Mahmud et al. (2015a), combined with the classification of drip rate data from the underlying drip sites (Mahmud et al., 2016), we determined previously that Chamber 1 (Figure 1b, c and d) is mostly dominated by matrix flow representing water flowing down and seeping through the rock matrix, characterised by both icicle-shape and

soda straw stalactites with slow drip rates of low variability. In contrast, Chamber 2 (Figure 1b and e) is typically controlled by fracture and combined flow, with high drip rates that are shown to vary over time depending upon the mode of water delivery to the preferential flow system. In fracture flow, water moves along the fracture orientation, forming curtain-shape stalactites in the direction of highest fracturing. Finally, combined flow is defined as the combination of conduit, matrix and fracture flow, resulting in a circular pattern of stalactite formation.

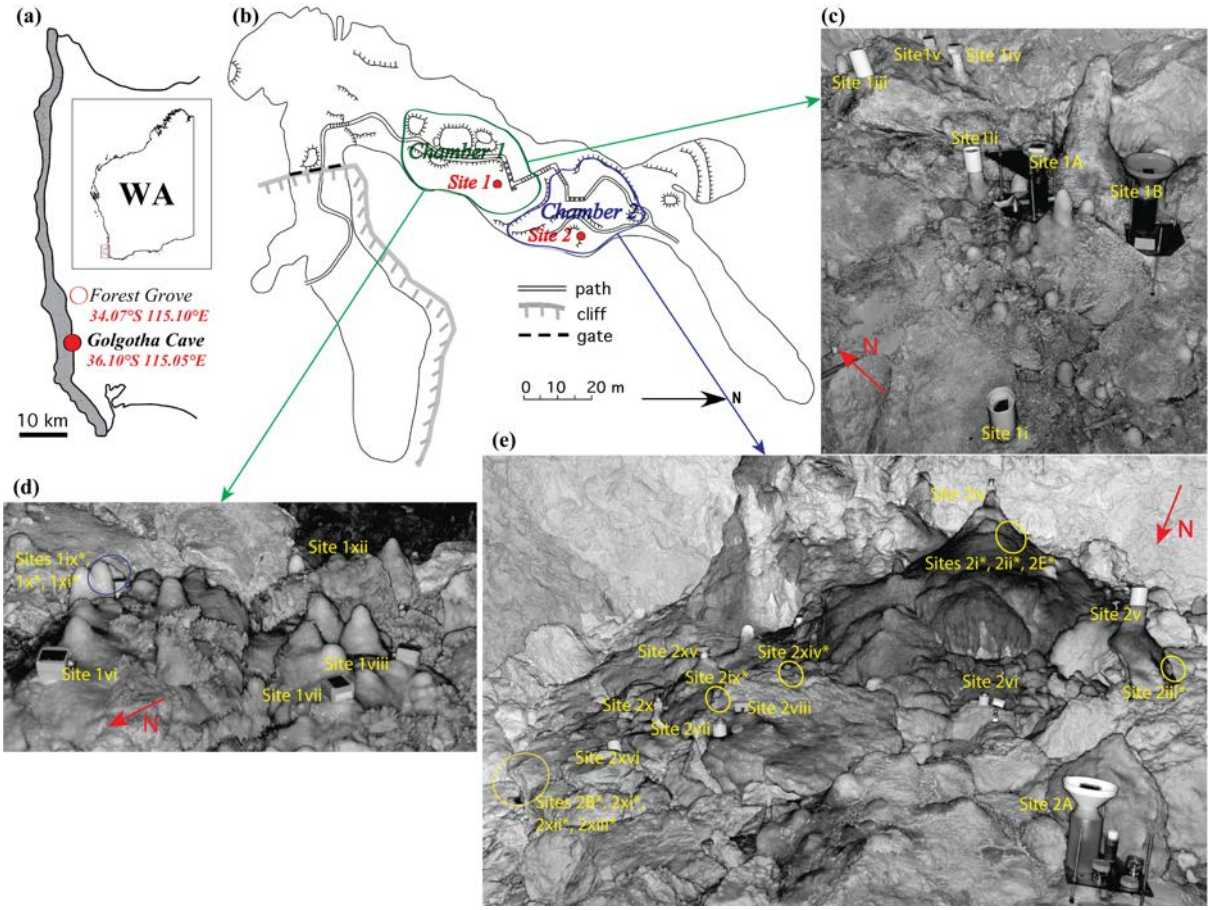

Figure 1: a) Coastal belt of SWWA (South-West Western Australia). (b) Golgotha cave plan view displaying both Chamber 1 (green marked area), which comprises Site 1, and Chamber 2 (blue marked area) containing Site 2. Average limestone thickness from cave ceiling to ground surface over Site 1 and 2 are 32.33 m and 40.24 m respectively. LiDAR scans of drip sites on: (c) Chamber 1 north floor, (d) Chamber 1 south floor and (e) Chamber 2 floor. The red arrows show the geographic orientation (c, d and e). * indicates the sites where the stalagmate loggers are not clearly visible in the LiDAR floor images as they are obscured by formations in front of them, however the approximate locations are marked in yellow circles. Additional scans of cave ceiling and photographs of underlying stalagmites are shown in Fig. 3 of Mahmud et al. (2016).

2.2 Climate and Meteorology

A comprehensive description of the climate at our study site has been presented in Mahmud et al. (2015a); Mahmud et al. (2016); Treble et al. (2013). To summarize, the site is a Mediterranean climate, associated with

wet winters and dry summers. Annual rainfall recorded at Forest Grove weather station (Figure 1a, 5 km away from the study site) is 1136.8 ± 184 mm, among which ~75% occurs between May and September, with an average daily maximum temperature variation from 16°C (in July) to 27°C (in February) (BoM, 2015). Typically, the peak rainfall begins in late autumn (May) and the wet season continues until end of September with a median monthly rainfall of ~100 mm (Mahmud et al., 2016). Each hydrological year is defined as April to March, as April has the lowest water budget (precipitation-evapotranspiration).

As reported in Mahmud et al. (2016), all hydrological years have water deficit during the dry season (October to April) and significant infiltration during the wet period (Mahmud et al., 2016). Low evaporative conditions during winter should permit increased infiltration to the caves, enhancing the drip discharge response to winter rainfall. The hydrological year 2012 had roughly similar annual rainfall of 1008.6 mm to the long-term annual mean, whereas 2013 was rather wet (total rainfall of 1239.8 mm) and 2014 was a relatively dry year with a total rainfall of 943.8 mm. Recorded rainfall was significantly above average in the 2013 hydrological year for various weather stations in Western Australia (BoM, 2015). Therefore, our site had a wetter winter in 2013 with an estimated annual recharge of 858.67 mm which is very much above average (ten year mean annual recharge is 564 mm).

2.3 Drip data acquisition and characteristics

Data acquisition and pre-processing has been previously described in Mahmud et al. (2016) and is concisely summarized here. Stalagmate drip loggers (www.driptych.com) were set up in approximate transects throughout the two large chambers from higher to lower ceiling elevation in 34 locations and are currently being monitored since August 2012. Each chamber has contrasting discharge, dune facies and karst features of Golgotha Cave (Figure 1). Data loggers were set to record continuously at 15 minute intervals. The notation used for site identification follows the same style as described in Mahmud et al. (2016), consisting of a numerical number (represents the chamber) and a letter/roman number (represents a drip site within the given chamber, with a letter indicates the sites having both manual and automatic drip counts and a roman number specifies the sites only having drip logger data). Based on the initial data screening of Mahmud et al. (2016), 29 sites are considered in the time series analysis although short periods of poor quality data were omitted if they were associated with changes in the mean and variability at the time of fieldwork. This impacted sites 1A, 1B, 2A, 2B, 2E as the logger was temporarily placed aside every 6 weeks in order to sample water from a collection bottle underneath the logger. Time series gaps are filled with synthetic data based on the drip statistics and correlation between drip rates. The processed drip rate time series for all the sites and three hydrological years from April 2012 to March 2015 were published in previous work of Mahmud et al. (2016).

As previously reported, drip rates in Chamber 1 are generally very low (the fastest drip rate was 25 drips per 15 mins) consistent with the predominance of matrix flow in this chamber. However, it is obvious that most drip loggers exhibit a clear response to the 2013 wet winter (Mahmud et al., 2016) and also indicate the substantial inter-annual variation in discharge between three hydrological years. All Chamber 1 drip sites (except site 1x) show a gradual drip rate decrease during summer 2012 to winter 2013 due to below average rainfall in 2012. Then after displaying the sudden increase in all drip discharges that express the 2013 wet winter, the drip rates

further reduce due to the dry 2014 hydrological year. This intra-annual variation is identified much greater than the inter-annual discharge variation of the drip sites, as previously observed in Baker et al. (1997). This suggests that high-resolution intra-annual drip rate data is helpful to obtain a complete picture of changing flow variability with recharge. The high resolution of the data sets includes precise characterization of the temporal behavior of an individual drip, illustrating the differences inherent to the drip sites.

In contrast, Chamber 2 drip rates present more variability between sites both in intra-annual and inter-annual discharges, except few very slow dripping sites (Mahmud et al., 2016). Of the Chamber 2 drips, the slow drip sites have the lowest coefficient of variations (COVs) and lowest discharges, indicative of matrix flow types (Mahmud et al., 2016). The timing of maximum drip rates is generally delayed in Chamber 2 versus Chamber 1: Chamber 1 drip rates typically peak in late spring/early summer (Oct-Dec) while Chamber 2 drips tend to peak a few months later (Dec-May), reflecting a longer water residence time. This may be a function of the thicker ceiling above Chamber 2 (40.24 versus 32.33 m) but also heterogeneity in flow paths to each chamber (Mahmud et al., 2015; Treble et al., 2016). Overall the drip response to the 2013 wet winter is amplified in Chamber 2 versus Chamber 1, consistent with the presence of greater fracture flow in Chamber 2 (Mahmud et al., 2015).

By applying morphological analysis of ceiling features acquired by LiDAR data, Mahmud et al. (2015a) distinguished three flow patterns (i.e. matrix flow, fracture flow, and a combination of conduit, fracture, and matrix flow) for the observed ceiling morphological features. All the drip sites were then characterized according to this flow classification in Mahmud et al. (2016), which is used here as a reference for clustering similar drip time series.

3 Methods

3.1 Hydrological classification of cave drips

Research involving automated drip monitoring systems is increasing, for example at Cathedral Cave in Wellington (Cuthbert et al., 2014) and Harrie Wood Cave in the Snowy Mountains, Yarrangobilly (Markowska et al., 2015). The variability of the drip discharge might not only be a function of discharge itself, but could also depend on the sampling frequency. We investigate this possibility by plotting the COV versus sampling interval (the original 15 mins and calculated by resampling the data at 1 hour, 1 day, 1 week and 1 month). COV is supposed to be artificially high at the high frequency of 15 mins because of sampling bias that artificially increases the noise. The resampling at low frequencies is only a way of smoothing out this noise. Using the optimum sampling frequency to minimize its effect on drip variability, we plot drip rate histograms to identify the response of drips between the flow classifications and the response to intra and inter-annual variability in infiltration. Finally, we summarize the mean discharge of drip sites in relation to the variability in discharge using the optimum sampling frequency. These are the same drip discharge parameters as used in the classification method proposed by Friederich and Smart (1982), Fairchild et al. (2006) and Baker et al. (1997) that were based on manual drip collection at low frequency.

3.2 Clustering of similar drip time series

We employed multi-dimensional scaling (MDS), which allows data dimensionality reduction i.e., mapping complex multidimensional data on a low-dimensional manifold. MDS is a technique that embeds a set of points in a low-dimensional space, so that the distances between the points resemble as closely as possible a given set of dissimilarities between the objects they represent (Birchfield and Subramanya, 2005). MDS requires a distance matrix to be computed, in which a single scalar number characterizes the similarity between any two time-series. In our case, each drip logger is an object and a specific distance between drip loggers is considered to characterize the similarity between any two loggers. It takes an input matrix giving dissimilarities between pairs of items and outputs a coordinate matrix whose configuration minimizes a loss function. MDS is also known as Principal Coordinates Analysis (PCoA). MDS operates on a distance or dissimilarity matrix (Pisani et al., 2016), which is different than principle-component analysis (PCA) that is based on a covariance matrix. Even if PCA and MDS methods can return the same results in specific contexts, MDS can be considered more general because it remains validity for non-euclidean distances, such as the distance matrix (d) chosen in this study. MDS is used to translate these distances into a configuration of points defined in an n-dimensional Euclidean space (Cox and Cox, 1994). A MDS results in a set of points arranged so that their corresponding Euclidean distances indicate the dissimilarities of the time series. According to Birchfield and Subramanya (2005) the basic steps of performing the MDS algorithm are:

i) Construct the distance matrix **D**: One key component in clustering is the function used to measure the temporal similarity (or distance) between any two time-series being compared. To define an appropriate measure of similarity between time series, we determine two factors: firstly, the offset (O) to match two time-series based on their maximum correlation, and secondly the complement of the correlation coefficient ($1-R$) between the time series (Jex et al. 2012). Initially, we compute the cross-correlation function, a measure of similarity of two time-series as a function of the displacement of one relative to the other. The cross-correlation function is an estimate of the covariance between two time-series, y_{1t} and y_{2t}, at lags $k = 0, \pm1, \pm2, ...$ The offset (O) is defined as the lag time based on the maximum correlation between two time-series. Next, we define R as the correlation coefficient with the time series being moved by the offset amount O to have maximum correlation coefficient. Both O and R are calculated to all $n(n-1)/2$ pairs of drip data, where n is the number of drip data. Here, we use the original recorded drip counts in 15 mins interval. The sampling bias discussed in section 3.1 is only affecting the drip variability, not the cluster analysis. Moreover, high resolution (15 mins interval) data are more suited for the cluster analysis because it allows better defining the cross-correlation between drips, as sometimes the offset of maximum correlation O might be less than a day. Finally, the distance matrix **D** is computed for each pair of loggers using the following equation (Jex et al. 2012):

$$\boldsymbol{D} = O(1 - R)$$

The distance matrix (**D**) is square, symmetric, and has dimension equal to the number of drip loggers.

ii) Compute the inner product matrix $B = -\frac{1}{2}J\boldsymbol{D}J$, where $J = I - \frac{1}{n}\mathbf{1}\mathbf{1}^T$ is the double-centering matrix and $\mathbf{1}$ is a vector of ones.

iii) Decompose B as $B = V\Lambda V^T$, where $\Lambda = \text{diag}\,(\lambda_1, \ldots, \lambda_n)$, the diagonal matrix of eigenvalues of B, and $V = [\mathbf{v}_1, \ldots, \mathbf{v}_n]$, the matrix of corresponding unit eigenvectors. Sort the eigenvalues in non-increasing order: $\lambda_1 \geq \cdots \geq \lambda_n \geq 0$.

iv) Extract the first p eigenvalues $\Lambda_p = \text{diag}\,(\lambda_1, \ldots, \lambda_p)$ and corresponding eigenvectors $V_p = [\mathbf{v}_1, \ldots, \mathbf{v}_p]$.

v) The corresponding Euclidean distances of the set of points, indicating the dissimilarities of the time series, are now located in the $n \times p$ matrix $X = \left[\mathbf{x}_1, \ldots, \mathbf{x}_p\right]^T = V_p {\Lambda_p}^{1/2}$.

The k-Means clustering algorithm is then used to divide these points into k clusters, which corresponds to a categorization of the drip data time series. k-means clustering, or Lloyd's algorithm (Lloyd, 1982), is a method of vector quantization that is popular for cluster analysis in data mining. k-means clustering aims to partition n observations into *k* clusters in which each observation belongs to the cluster with the nearest mean, serving as a prototype of the cluster. Here we use 4 clusters as this was the number of flow categories identified by Mahmud et al. (2016). The algorithm proceeds as follows:

i) Choose *k* initial cluster centers (*centroid*): Here, we use *k*=4 clusters as this was the number of flow categories identified by Mahmud et al. (2016).

ii) Compute point-to-cluster-centroid distances of all observations to each centroid. There are two steps to follow: first assign each observation to the cluster with the closest centroid. Then individually assign observations to a different centroid if the reassignment decreases the sum of the within-cluster, sum-of-squares point-to-cluster-centroid distances.

iii) Compute the average of the observations in each cluster to obtain *k* new centroid locations.

iv) Repeat steps 2 and 3 until cluster assignments do not change, or the maximum number of iterations is reached.

4 Results and Discussion

4.1 Determining the relationship between sampling frequency and drip discharge COV

We test the variability of drip discharge COV with the sampling frequency in Figure 2, to find the optimum sampling frequency that minimizes sampling artifacts while maximizing the capture of natural variability. For high discharge, COV increases with sampling frequency, which we explain by the smaller sampling interval better capturing the actual drip variability. For low discharges, COV also increases with sampling frequency, which we explain by the variability introduced due to drip rates being less than the sampling frequency. From the data presented in Figure 2, we can conclude that for both chambers and to compare all different types of

flow, a sampling frequency of 1 day gives the minimum COV, which does not change significantly with a finer sampling frequency. Therefore, we use a sampling frequency of 1 day that minimizes sampling artifacts while maximizing the capture of natural variability. For Golgotha Cave, this would be to sum the 15 minutes drip rates over a 1-day period. This optimized sampling frequency is used to plot the histograms (section 4.2), ACFs (supplementary section S1) and examine the drip discharge behavior with drip variability for various flow types (section 4.3).

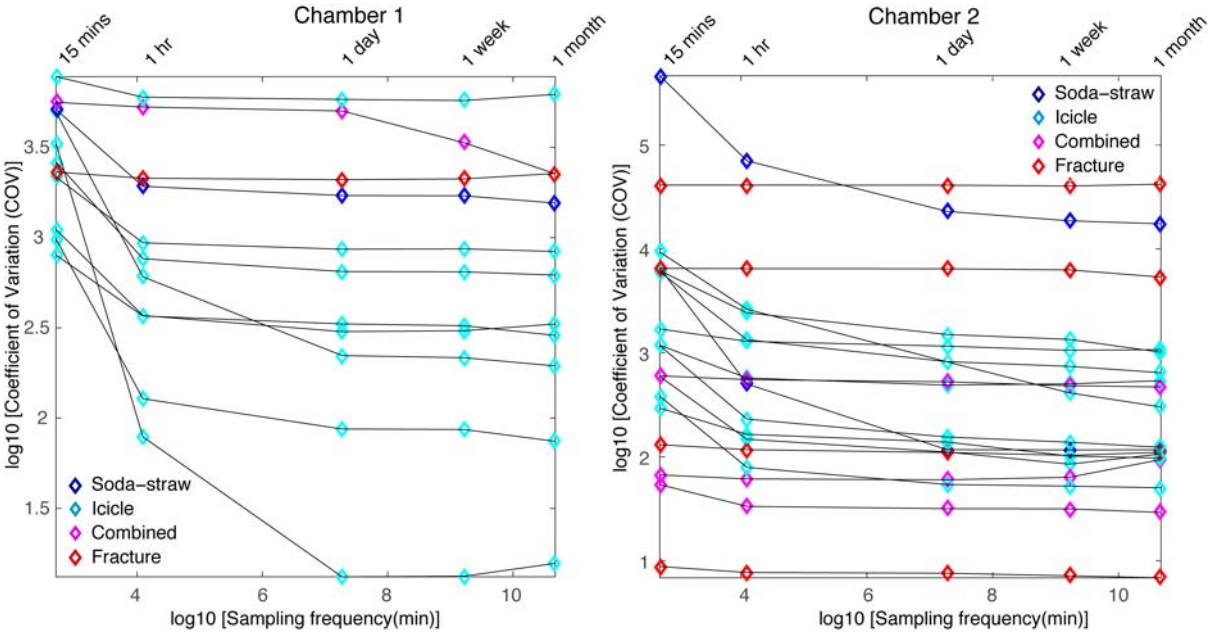

Figure 2: Optimum sampling frequency that minimizes sampling artifacts while maximizing the capture of natural variability.

4.2 Drip rate frequency distributions

Figure 3 shows the drip rate histograms for representative drip sites and different flow categories with optimum sampling frequency of 1-day. Drip sites are organized from lowest to highest discharge in each flow classification (Mahmud et al., 2016). Slow dripping soda-straw flows (e.g. sites 2xi, 2iii and 1v) show variation of drips with seasonality and the response to wetter recharge period with an approximate six-month lag, which suggests the drip water is supplied from storage in the limestone formation. Among these, site 1v displays the response to recharge in much shorter duration, the 6 months following 2013 recharge and then a shift to lower flow rates which may represent flow poaching. The histograms for icicle and combined flow systems represent unimodal skewed to bimodal distributions, indicating the shift to higher drip rates in response to the wetter 2013 hydrological year (except site 2xiii, which shows a shift to lower drip rates). The rest of the fracture sites show bimodal or multimodal distributions. With the limited temporal scale of the analysis, it seems that the histograms with skewed distributions represent the consequences of wetter 2013 hydrological year. These skewed distributions seem to have higher drip rate response to the drier 2014-15 period rather than the earlier normal/wetter years. This clearly denotes potential refilling of storage within the system during the 2013 wet winter, and later supplying drip water in 2014-15 seasons. The presence of ample storage in the karst system is

also supported by the autocorrelation functions (ACFs) discussed in supplementary section S1. In contrast, the bimodal distribution of site 2viii indicates the drip response to the annual cycle of wet and dry seasons of each hydrological year with an approximate six-month lag. Several bimodal (e.g. site 1x) and multimodal (e.g. sites 2xvi, 2vi) distributions, characterize as fracture flow, also distinguishes the dry period of 2012 - 2013 (having low drip rates) from the later period of 2013 wet winter (with high drip rates).

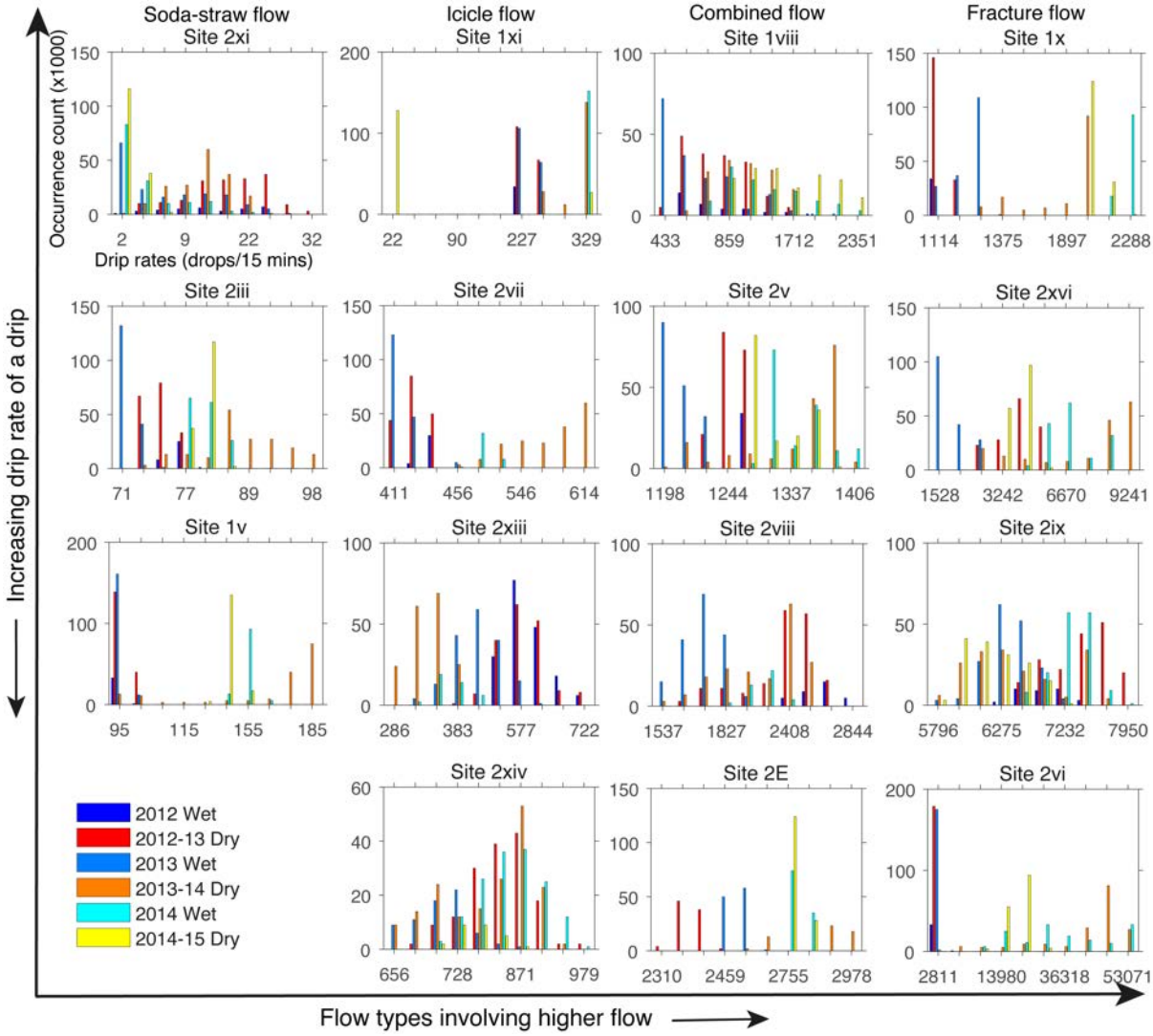

Figure 3: Histogram plots of both chambers drip data according to four flow types identified by Mahmud et al. (2016). Each histogram represents the frequencies of the drip counts per day (The axes labels are shown in the first histogram). Bin size is uniform for all plots and the external tick marks in x-axes delineates the bin intervals. The legend shows all the seasons over the monitoring period (blue to cyan for wet seasons: April to September and red to yellow for dry seasons: October to March, with the color gradually shifting for different years). The 2012 wet season experienced similar rainfall to the long-term annual mean, whereas 2013 was rather wet and 2014 was a relatively dry year. Histogram data for all sites appear in Supplementary Figure S1.

4.3 Hydrological classification of cave drips

We examine the hydrological behavior of the drips at daily resolution with respect to mean discharge and flow variation in Figure 4. The boundary lines drawn on this figure are based on the flow classification from the morphological analysis of Mahmud et al. (2015b). It is clear from Figure 4 that there is no relationship between COV and flow-type. One soda-straw discharge (site 2xi) has a seasonal dryness, a very low discharge, and a very high coefficient of variation due to its irregular dripping. Otherwise, nearly all soda-straw flow, icicle flow, combined flow and fracture flow drips have COV <60%, with the exception of one fracture flow site showing the highest COV (Figure 4). But in general, there is little difference in the COV between classification types, probably reflecting the ample storage (supplementary section S1) due to the dominance of primary porosity at this cave. We do not clearly observe increasing variability with decreasing discharge within similar flow type, in contrast to other studies from older, fractured rock limestones (Smart and Friederich, 1987; Baldini et al., 2006; Baker et al., 1997). This shows that Golgotha Cave drip sites do not fit within the drip classification method proposed by Smart and Friederich (1987) and Baker et al. (1997), which were based on manual drip counts with limited number of intermittent drip sites. Moreover, we utilize drip data from a cave with primary porosity, capturing the full range of flow types from matrix through to fracture, whereas the previous classifications only captured slow vs fast drips that were likely dominated by fracture flow paths given the host rock setting.

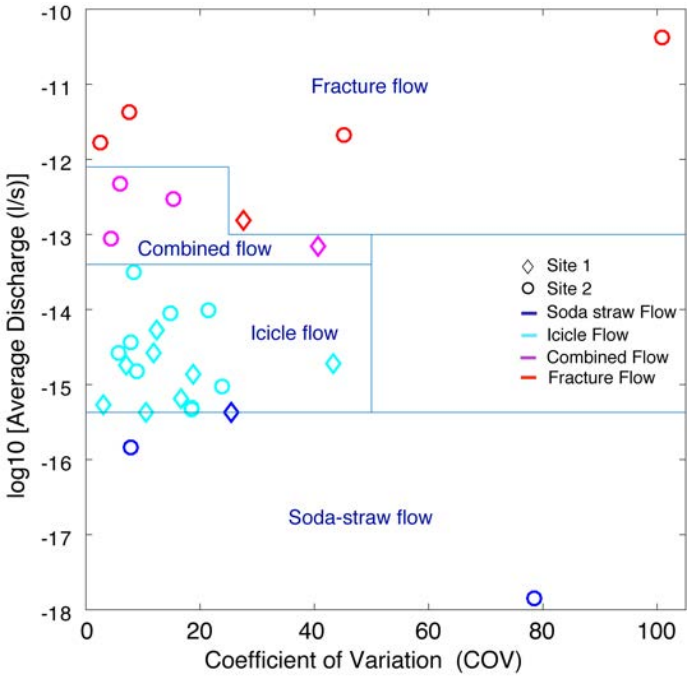

Figure 4: Hydrological behaviour of drip sites expressed in terms of daily mean discharge versus daily discharge variability calculated from the automatic drip rate data for three hydrological years. Measured drip rates are converted to volume units assuming a drip volume of 0.1433 ml (Genty and Deflandre, 1998). Blue lines and symbols reflect flow classification given in Mahmud et al. (2015).

4.4 Clustering of similar drip time series

The clustering results are overlain upon the chamber ceiling images in Figure 5 and also summarized in Tables 1 and 2 with the average drip discharges and LiDAR classified flow type taken from Mahmud et al. (2015a); Mahmud et al. (2016). Average drip discharges are calculated from the 15-minute drip rates of Mahmud et al (2016). As mentioned above, drip logger time series are deemed similar if they are well correlated and only have a small offset with each other, and so these time series should cluster together. Most of the drip sites that are identified as matrix flow (soda-straw and icicle flow) cluster together in C1. However, three of the icicle flow sites with drip rate greater than 4 per 15 minutes fall in C2. The combined flow category and the fracture type usually cluster in C3 and C4 respectively. Therefore we observe that our clustering generally agrees with the morphology-based flow classification of Mahmud et al. (2016). Few of the flow classes show exceptions, for example site 2vi is a fracture type flow and cluster in C1. This site has really high discharge with high variability, showing irregular drip rate.

Table 1: MDS cluster groups with statistical properties of Chamber 1 drip data.

Site/Stalagmate	MDS Cluster Group	Average drip discharge (l/yr)	Flow type (LiDAR-based)
1A	1	19.8	Icicle
1B	1	12.6	Icicle
1i	1	6.6	Icicle
1ii	1	11.2	Icicle
1iii	1	8.1	Icicle
1v	1	6.7	Soda-straw
1vi	1	7.4	Icicle
1viii	2	60.9	Combined
1ix	1	14.8	Icicle
1x	3	86.2	Fracture
1xi	1	12.7	Icicle

Table 2: MDS cluster groups with statistical properties of Chamber 2 drip data

Site/Stalagmate	MDS Cluster Group	Average drip discharge (l/yr)	Flow type (LiDAR-based)
2A	1	9.4	Icicle
2B	1	17.1	Icicle
2E	3	140.3	Combined
2i	4	243.0	Fracture
2iii	1	4.2	Soda-straw
2iv	1	14.6	Icicle
2v	3	67.8	Combined
2vi	1	985.0	Fracture
2vii	2	25.0	Icicle
2viii	3	113.8	Combined
2ix	4	360.2	Fracture
2x	1	7.0	Icicle
2xi	1	0.6	Soda-straw
2xiii	2	26.2	Icicle
2xiv	2	42.8	Icicle
2xv	1	11.6	Icicle
2xvi	3	266.9	Fracture
2xvii	1	7.0	Icicle

One consistent feature that appears from the cluster analysis of Figure 5 is the spatial homogeneity of the clusters in Chamber 1, suggesting that they are spatially connected, or that their flow paths are connected to the same hydrological domain (the karst matrix), and supporting the overall dominant matrix flow patterns (both soda-straw and icicle). Chamber 2 presents a completely different situation, where it is obvious that drip sites can have similar behavior (well correlated together with a small lag), and be spatially distinct features, separated by spans of approximately 6 meters (Figure 5). In particular, clusters 3 and 4 are spatially scattered, representing the presence of fractures and combined flow systems throughout the chamber ceiling. This indicates an overall strong heterogeneity of the flow paths between the surface and the cave for Chamber 2. Hence, in Chamber 2 we expect flow paths to be more complex with routing between multiple stores and interconnected fracture networks potentially resulting in non-linear response to infiltration. This is supported by dripwater $\delta^{18}O$ data for this chamber (Treble et al., 2013).

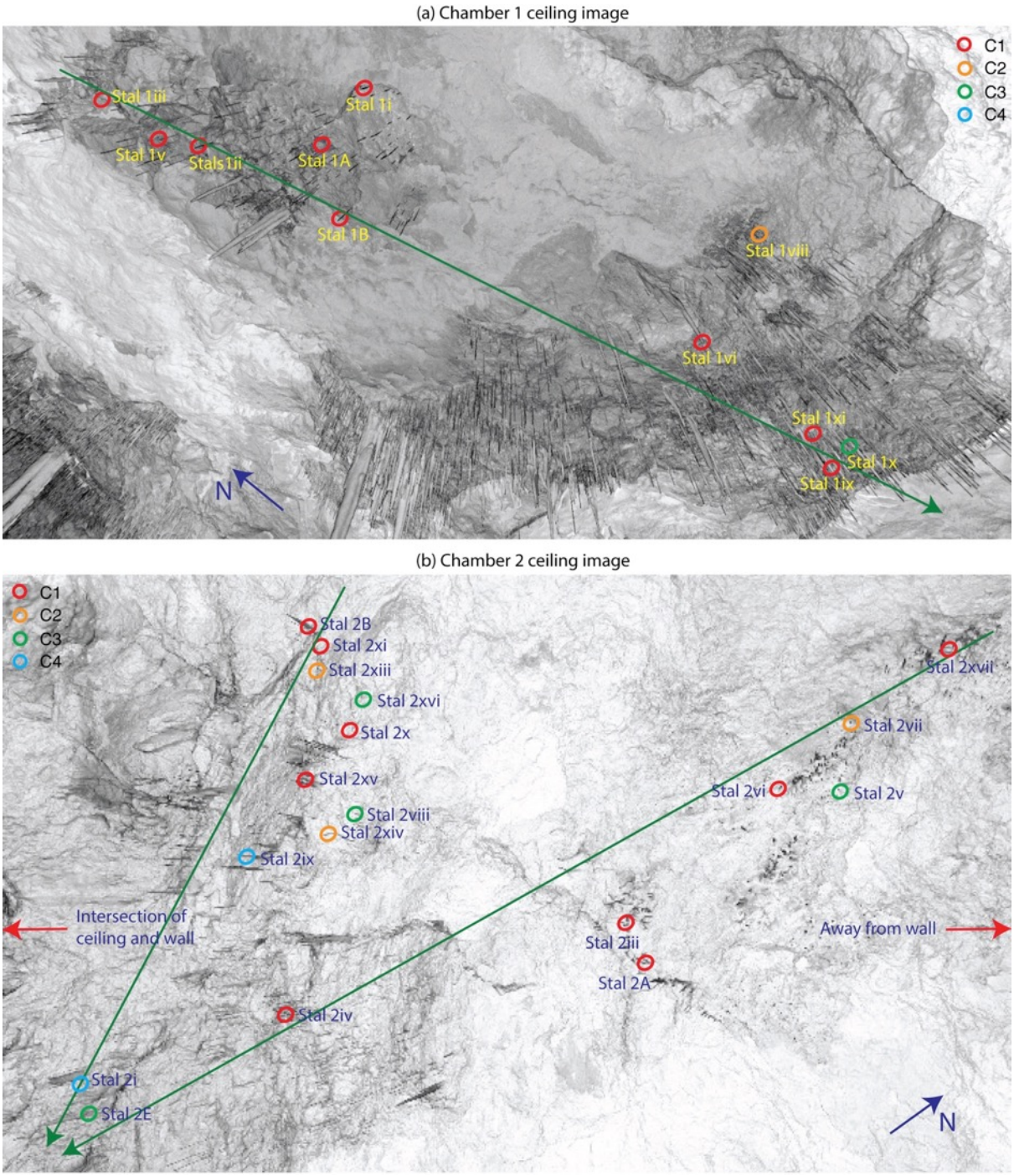

Figure 5: Cluster group plot overlain upon the cave ceiling for both chambers. The ceiling images are captured by LiDAR and the circles represent the ceiling locations of stalactites dripping on various stalagmates in both chambers (shown in Figure 1). The colour of the circles indicates individual MDS cluster group. The blue arrows in both Figures show the geographic orientation and the green arrows represent the approximate transects throughout the chambers from higher to lower ceiling elevation.

5 Implications of the findings and future research

Starting with the time-series analysis, this research presents a methodology that can be applied globally for drip logger data. The results show that some data-integration is necessary to avoid artefacts from slow drip sites. For

sites where there is significant matrix flow, our study has demonstrated that the Smart and Friederich classification is not appropriate. Therefore, this study has presented alternative hydrological classification schemes that are suitable for cave sites that include matrix flow. The times series approach adopted in this study also opens the way for improved analysis and classification of hydrology time series in general i.e. tests for histogram, autocorrelation, cluster analysis, and all of these will certainly benefit our understanding of the hydrology of karst systems.

In this study, we also extend the analysis of drip time series to multiple sites, whereby we take advantage of the ensemble of loggers to extract common properties by clustering, which would not be possible with single site analysis. The results show that by considering multiple simultaneous time series, one can make better inferences about water flow and unsaturated zone properties. The main impact is to recommend the use of spatial networks of loggers over individual loggers. It should be noted that currently, most researchers deploy only a few loggers to understand the flow to individual sites. This study also proposes a possible methodology for the analysis of such datasets.

Regarding application of our findings, we believe that our methodology based on drip logger datasets can provide direct evidence of deep drainage, and therefore the timing of diffuse recharge, which could be used for basic model calibration. Spatial drip data (possibly combined with Lidar) is beneficial to infer flow types (e.g. the proportion of fracture vs matrix, etc.) which could be used for model configuration to produce realistic karst recharge (Hartmann et al., 2012), and hence large-scale groundwater estimation (Hartmann et al., 2015). Another potential application is the integration of flow types in groundwater models through inverse modelling. Such data could also be used to constrain water isotope model configurations used for forward modelling speleothem $\delta^{18}O$ (Bradley et al., 2010; Treble et al., 2013). Overall, the findings of this work will definitely provide a better understanding of processes that control vadose zone flow and transport processes, which would ultimately help develop approaches to incorporate these processes into simulation models (Hartmann and Baker, 2017).

The analysis, presented here and combined with the findings of our previous two papers (Mahmud et al., 2015a; Mahmud et al., 2016), provides valuable information for paleoclimatologists and geochemists wishing to sample stalagmites. While these studies have characterised Golgotha Cave, they could be applied to any other cave system. In our previous work, we have: 1) devised a classification for flow-type based on stalactite morphology (Mahmud et al., 2015a); 2) quantified the recharge response of each flow type to infiltration (Mahmud et al., 2016) and; 3) combined the findings of points 1-2 to estimate the total volume of cave discharge; 4) compared cave discharge with infiltration to estimate the total recharge volume and identify highly focused areas of recharge (Mahmud et al., 2016). The current study has further developed the spatial and temporal statistical relationships between the flow sites, permitting both quantification and visualisation of the hydrology between the ground surface and the cave ceiling. More generally, these studies illustrate the heterogeneity between flow sites and what causes this, as well as putting forth methods that can be applied to any cave system to better understand diffuse recharge and paleoclimate records from speleothems.

We further propose some ideas for future research that have evolved from this study:

a) Combining a drip logger network with a surface weather station and soil moisture network to constrain the water balance in hydrological models. Additionally, employing sap flow meters could allow constraining tree water use.

b) Combining the logger network, which constrains diffuse recharge, to boreholes measuring groundwater level to understand the relative importance of diffuse and river recharge.

c) Combining cave drip logger data with surface geophysics data to track water movement.

6 Conclusion

Cave drip water response to surface climatic conditions is often complex due to numerous interacting drip routes with varying response times (Baldini et al., 2006). This study explores the relationship between drip water and rainfall in a SW Australian karst, where both intra- and inter-annual hydrological variations are strongly controlled by seasonal variations in recharge. The multi-year drip response data capture the inter-annual drip water variability that are likely to be greater than intra-annual variability as suggested by Baker et al. (1997). Building on the studies of Mahmud et al. (2015a) and Mahmud et al. (2016), we further analyse a set of statistical properties of three hydrological years of drip data under varying precipitation rates. We test the relationship between drip discharge variability and drip data sampling frequency to determine the optimum sampling frequency that maximizes the capture of natural variability with minimum sampling artifacts. Using the daily optimum sampling frequency, the histogram distributions of various drip data time series illustrate the differences between the flow classifications. Most of the drip sites show persistent autocorrelation for at least a month. The hydrological behavior of the drips is examined with respect to mean discharge and the flow types similar to the classification method proposed by previous researchers (Smart and Friederich, 1987; Baldini et al., 2006; Baker et al., 1997). The drip sites at Golgotha Cave described in this study do not fit within the drip classification method proposed by Smart and Friederich (1987) and Baker et al. (1997). These previous studies were based on manual drip counts with limited number of intermittent drip sites. Here we overcome these limitations with automated drip monitoring system.

Finally, we apply a well-developed clustering method to determine the degree of similarity between drip time series. The clustering indicates one dominating group: C1 (characterized by matrix flow type) with very slow continuous drip discharge indicating matrix porosity in the thick limestone formation. This finding concurs with the observed cave chamber morphology and lithology. Moreover, the cluster analysis agrees with the flow classification of Mahmud et al. (2016) by grouping similar flow type in one single cluster. Overall this study establishes a novel way to find consistent characterization of cave hydrology, which can be obtained by performing together both methodologies of Mahmud et al. (2015a) and Jex et al. (2012). It relies on a metric that defines drip logger time series as similar if they are well correlated and only have a small offset with one another, and therefore these time series should cluster together. The MDS analysis supports this hypothesis and moreover, displays the spatial patterns of the flow paths between the surface and the cave chambers. This technique shows potential to classify, quantify and visualise the observed relationships between infiltration through the fractured limestone rocks and surface climate inputs.

Over the last decade, the automation of cave drip water hydrology measurements has permitted the routine generation of continuous hydrological time series for the first time. This study demonstrates a complete methodology for such datasets, which will help better characterize karst drip water hydrogeology and understand the relationship between drip hydrology and surface climate at any cave site where such measurements are made. We demonstrate that the analysis of the time series produced by cave drip loggers generates useful hydrogeological information that can be applied generally, beyond the example presented here. The time series behaviour integrates a variety of characteristics that combine the properties of the epikarst (storage), fracture configuration, and recharge. The clustering approach can identify which drip behaviour are related to these cave characteristics, and their spatial relationship. Most importantly, information on cave characteristics can now be gathered at a very low cost in terms of measurement and time.

Acknowledgment

This paper is based on work supported by UNSW Australia, UNSW Connected Waters Initiative Research Center and the National Centre for Groundwater Research and Training. The authors wish to thank individuals (Andy Spate, Alan Griffiths, Liz McGuire, Carolina Paice, Anne Wood, Monika Markowska and others) who assisted in data acquisition at Golgotha cave site.

References

Arbel, Y., Greenbaum, N., Lange, J., and Inbar, M.: Infiltration processes and flow rates in developed karst vadose zone using tracers in cave drips, Earth Surface Processes and Landforms, 35, 1682-1693, 10.1002/esp.2010, 2010.

Baker, A., Barnes, W. L., and Smart, P. L.: Variations in the discharge and organic matter content of stalagmite drip waters in Lower Cave, Bristol, Hydrological Processes, 11, 1541-1555, 10.1002/(sici)1099-1085(199709)11:11<1541::aid-hyp484>3.0.co;2-z, 1997.

Baldini, J. U. L., McDermott, F., and Fairchild, I. J.: Spatial variability in cave drip water hydrochemistry: Implications for stalagmite paleoclimate records, Chemical Geology, 235, 390-404, http://dx.doi.org/10.1016/j.chemgeo.2006.08.005, 2006.

Birchfield, S. T., and Subramanya, A.: Microphone Array Position Calibration by Basis-Point Classical Multidimensional Scaling, IEEE Transactions on Speech and Audio Processing, 13, 1025-1034, 10.1109/TSA.2005.851893, 2005.

BoM: Climate Data Online (Station 9547), Bureau of Meteorology Melbourne. http://www.bom.gov.au/climate/data/ (Accessed 26-08-2014), in, 2015.

Borg, I., and Groenen, P.: Modern multidimensional scaling: theory and applications, Springer, New York, 614 pp., 1997.

461 Bradley, C., Baker, A., Jex, C. N., and Leng, M. J.: Hydrological uncertainties in the modelling of cave drip-
462 water δ18O and the implications for stalagmite palaeoclimate reconstructions, Quaternary Science Reviews, 29,
463 2201-2214, 2010.

464 Brooke, B. P., Olley, J. M., Pietsch, T., Playford, P. E., Haines, P. W., Murray-Wallace, C. V., and Woodroffe,
465 C. D.: Chronology of Quaternary coastal aeolianite deposition and the drowned shorelines of southwestern
466 Western Australia – a reappraisal, Quaternary Science Reviews, 93, 106-124,
467 http://dx.doi.org/10.1016/j.quascirev.2014.04.007, 2014.

468 Collister, C., and Mattey, D.: Controls on water drop volume at speleothem drip sites: An experimental study, J.
469 Hydrol., 358, 259-267, http://dx.doi.org/10.1016/j.jhydrol.2008.06.008, 2008.

470 Cox, T., and Cox, M.: Multidimensional scaling, Chapman and Hall, London, 213 pp., 1994.

471 Cuthbert, M. O., Baker, A., Jex, C. N., Graham, P. W., Treble, P. C., Andersen, M. S., and Ian Acworth, R.:
472 Drip water isotopes in semi-arid karst: Implications for speleothem paleoclimatology, Earth Planet. Sci. Lett.,
473 395, 194-204, http://dx.doi.org/10.1016/j.epsl.2014.03.034, 2014.

474 Fairchild, I. J., Tuckwell, G. W., Baker, A., and Tooth, A. F.: Modelling of dripwater hydrology and
475 hydrogeochemistry in a weakly karstified aquifer (Bath, UK): Implications for climate change studies, J.
476 Hydrol., 321, 213-231, http://dx.doi.org/10.1016/j.jhydrol.2005.08.002, 2006.

477 Ford, D., and Williams, P.: Karst Hydrogeology and Geomorphology, Wiley, 576 pp., 2007.

478 Friederich, H., and Smart, P. L.: The classification of autogenic percolation waters in karst aquifers: A study in
479 G.B. cave, Mendip Hills, England, Proceedings of the University of Bristol Speleological Society, 1982, 143–
480 159, 1982.

481 Genty, D., and Deflandre, G.: Drip flow variations under a stalactite of the Pere Noel cave (Belgium). Evidence
482 of seasonal variations and air pressure constraints, J. Hydrol., 211, 208-232, 1998.

483 Hartmann, A., Lange, J., Weiler, M., Arbel, Y., and Greenbaum, N.: A new approach to model the spatial and
484 temporal variability of recharge to karst aquifers, Hydrol. Earth Syst. Sci., 16, 2219-2231, 10.5194/hess-16-
485 2219-2012, 2012.

486 Hartmann, A., Gleeson, T., Rosolem, R., Pianosi, F., Wada, Y., and Wagener, T.: A large-scale simulation
487 model to assess karstic groundwater recharge over Europe and the Mediterranean, Geosci. Model Dev., 8, 1729-
488 1746, 10.5194/gmd-8-1729-2015, 2015.

Hartmann, A., and Baker, A.: Modelling karst vadose zone hydrology and its relevance for paleoclimate reconstruction, Earth-Science Reviews, 172, 178-192, http://dx.doi.org/10.1016/j.earscirev.2017.08.001, 2017.

Jex, C. N., Mariethoz, G., Baker, A., Graham, P., Andersen, M., Acworth, I., Edwards, N., and Azcurra, C.: Spatially dense drip hydrological monitoring and infiltration behaviour at the Wellington Caves, South East Australia, International Journal of Speleology, 41, 283–296, 2012.

Klimchouk, A.: Towards defining, delimiting and classifying epikarst: Its origin, processes and variants of geomorphic evolution, Speleogenesis and Evolution of Karst Aquifers, 2, 1-13, 2004.

Kurtzman, D., Navon, S., and Morin, E.: Improving interpolation of daily precipitation for hydrologic modelling: spatial patterns of preferred interpolators, Hydrological Processes, 23, 3281-3291, 10.1002/hyp.7442, 2009.

Lange, J., Greenbaum, N., Husary, S., Ghanem, M., Leibundgut, C., and Schick, A. P.: Runoff generation from successive simulated rainfalls on a rocky, semi-arid, Mediterranean hillslope, Hydrological Processes, 17, 279-296, 10.1002/hyp.1124, 2003.

Liao, T. W.: Clustering of time series data-a survey, Pattern Recogn., 38, 1857-1874, 10.1016/j.patcog.2005.01.025, 2005.

Lloyd, S.: Least squares quantization in PCM, IEEE Transactions on Information Theory, IT-28, 129-137, 1982.

Mahmud, K., Mariethoz, G., Pauline, C. T., and Baker, A.: Terrestrial Lidar Survey and Morphological Analysis to Identify Infiltration Properties in the Tamala Limestone, Western Australia, Selected Topics in Applied Earth Observations and Remote Sensing, IEEE Journal of, 8, 4871 - 4881, 10.1109/JSTARS.2015.2451088, 2015a.

Mahmud, K., Mariethoz, G., Pauline, C. T., and Baker, A.: Terrestrial Lidar Survey and Morphological Analysis to Identify Infiltration Properties in the Tamala Limestone, Western Australia, Selected Topics in Applied Earth Observations and Remote Sensing, IEEE Journal of, In Press, 10.1109/JSTARS.2015.2451088, 2015b.

Mahmud, K., Mariethoz, G., Baker, A., Treble, P. C., Markowska, M., and McGuire, L.: Estimation of deep infiltration in unsaturated limestone environments using cave LiDAR and drip count data, Hydrol. Earth Syst. Sci., 20, 359-373, 10.5194/hess-20-359-2016, 2016.

Mariethoz, G., Baker, A., Sivakumar, B., Hartland, A., and Graham, P.: Chaos and irregularity in karst percolation, Geophys. Res. Lett., 39, n/a-n/a, 10.1029/2012gl054270, 2012.

516 Markowska, M., Baker, A., Treble, P. C., Andersen, M. S., Hankin, S., Jex, C. N., Tadros, C. V., and Roach, R.:
517 Unsaturated zone hydrology and cave drip discharge water response: Implications for speleothem paleoclimate
518 record variability, Journal of hydrology, 529, 662–675, http://dx.doi.org/10.1016/j.jhydrol.2014.12.044, 2015.

519 Pisani, P., Caporuscio, F., Carlino, L., and Rastelli, G.: Molecular Dynamics Simulations and Classical
520 Multidimensional Scaling Unveil New Metastable States in the Conformational Landscape of CDK2, PLoS
521 ONE, 11, 1-22, 10.1371/journal.pone.0154066, 2016.

522 Scheidt, C., and Caers, J.: Representing spatial uncertainty using distances and kernels, Math. Geosci., 41, 397-
523 419, 2009.

524 Smart, P. L., and Friederich, H.: Water movement and storage in the unsaturated zone of a maturely karstified
525 carbonate aquifer, Proceedings of the conference on Environmenatl Problems in Karst Terranes and their
526 Solutions, Dublin, Ohio, 1987, 59-87,

527 Smith, A. J., Massuel, S., and Pollock, D. W.: Geohydrology of the Tamala Limestone Formation in the Perth
528 Region: Origin and Role of Secondary Porosity, 63, 2012.

529 Treble, P. C., Bradley, C., Wood, A., Baker, A., Jex, C. N., Fairchild, I. J., Gagan, M. K., Cowley, J., and
530 Azcurra, C.: An isotopic and modelling study of flow paths and storage in Quaternary calcarenite, SW Australia:
531 implications for speleothem paleoclimate records, Quaternary Science Reviews, 64, 90-103,
532 http://dx.doi.org/10.1016/j.quascirev.2012.12.015, 2013.

533 Treble, P. C., Fairchild, I. J., Griffiths, A., Baker, A., Meredith, K. T., Wood, A., and McGuire, E.: Impacts of
534 cave air ventilation and in-cave prior calcite precipitation on Golgotha Cave dripwater chemistry, southwest
535 Australia, Quaternary Science Reviews, 127, 61–72, http://dx.doi.org/10.1016/j.quascirev.2015.06.001, 2015.

536 Treble, P. C., Fairchild, I. J., Baker, A., Meredith, K. T., Andersen, M. S., Salmon, S. U., Bradley, C., Wynn, P.
537 M., Hankin, S. I., Wood, A., and McGuire, E.: Roles of forest bioproductivity, transpiration and fire in a nine-
538 year record of cave dripwater chemistry from southwest Australia, Geochimica et Cosmochimica Acta, 184,
539 132-150, http://dx.doi.org/10.1016/j.gca.2016.04.017, 2016.

540 Williams, P. W.: The role of the subcutaneous zone in karst hydrology, J. Hydrol., 61, 45-67,
541 http://dx.doi.org/10.1016/0022-1694(83)90234-2, 1983.

542

Hydrological characterization of cave drip waters in a porous limestone: Golgotha Cave, Western Australia

Kashif Mahmud[1], Gregoire Mariethoz[2], Andy Baker[3], Pauline C. Treble[4]

Supplementary Information

Figure S1: Histogram plots of all drip sites. Each histogram represents the frequencies of the drip counts per day (The axes labels are shown in the first histogram). Bin size is uniform for all plots and the external tick marks in x-axes delineates the bin intervals. The legend shows all the seasons over the monitoring period (blue to cyan for wet seasons: April to September and red to yellow for dry seasons: October to March, with the color gradually shifting for different years). The 2012 wet season experienced similar rainfall to the long-term annual mean, whereas 2013 was rather wet and 2014 was a relatively dry year.

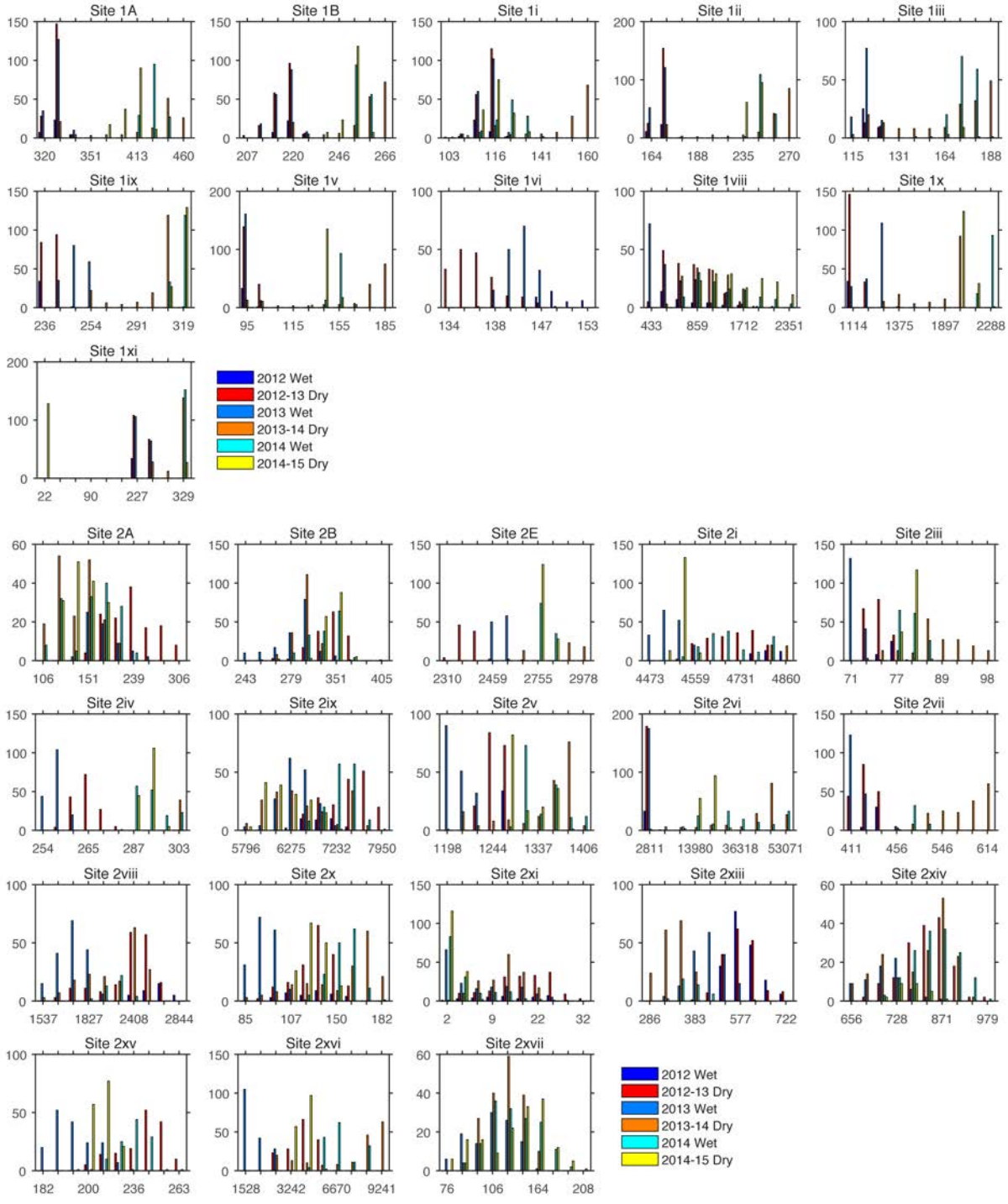

Section S1: Autocorrelation functions (ACFs)

We investigate the use of ACFs to analyze drip behavior using the optimum sampling frequency of 1-day and until lags of 365 days. We do not find significant yearly autocorrelation with this limited 3 years of data. In some drips, a negative correlation occurred, but it is very insignificant and no physical process can explain a negative yearly correlation. Therefore, we plot ACFs in Figure S2 for different flow categories with the optimum sampling frequency of 1-day and lag time of 200 days. All sites have an autocorrelation that persists for at least a month, and often much longer. However, there is no relationship between the strength of correlation or the time period of the autocorrelation with the LiDAR-based flow type (Mahmud et al., 2016). This indicates the presence of ample storage in the system, supplying all stalactite types.

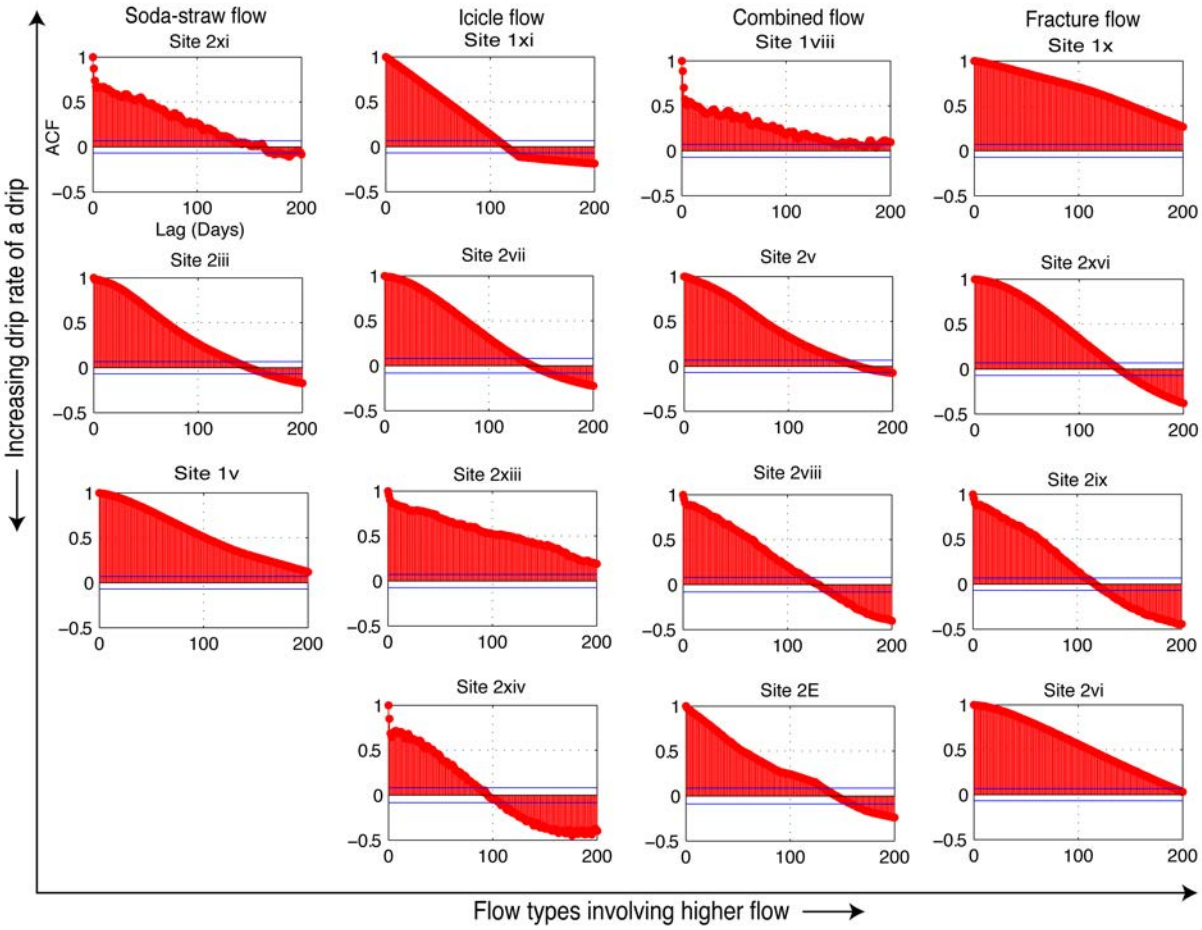

Figure S2: Autocorrelation functions of both chambers drip data according to flow classification of Mahmud et al. (2016). X- and Y-axis of individual plots represents the lag (in days) and ACF respectively (The axes labels are shown in the first ACF plot).